

ANALYTICAL AND EXPERIMENTAL STUDY OF A STANDING TORUS WITH NORMAL LOADS

Michael J. Mack, Jr.
Hewlett-Packard Co.

Daniel E. Hill
Deere & Company, Technical Center

Joseph R. Baumgarten
Department of Mechanical Engineering
Iowa State University

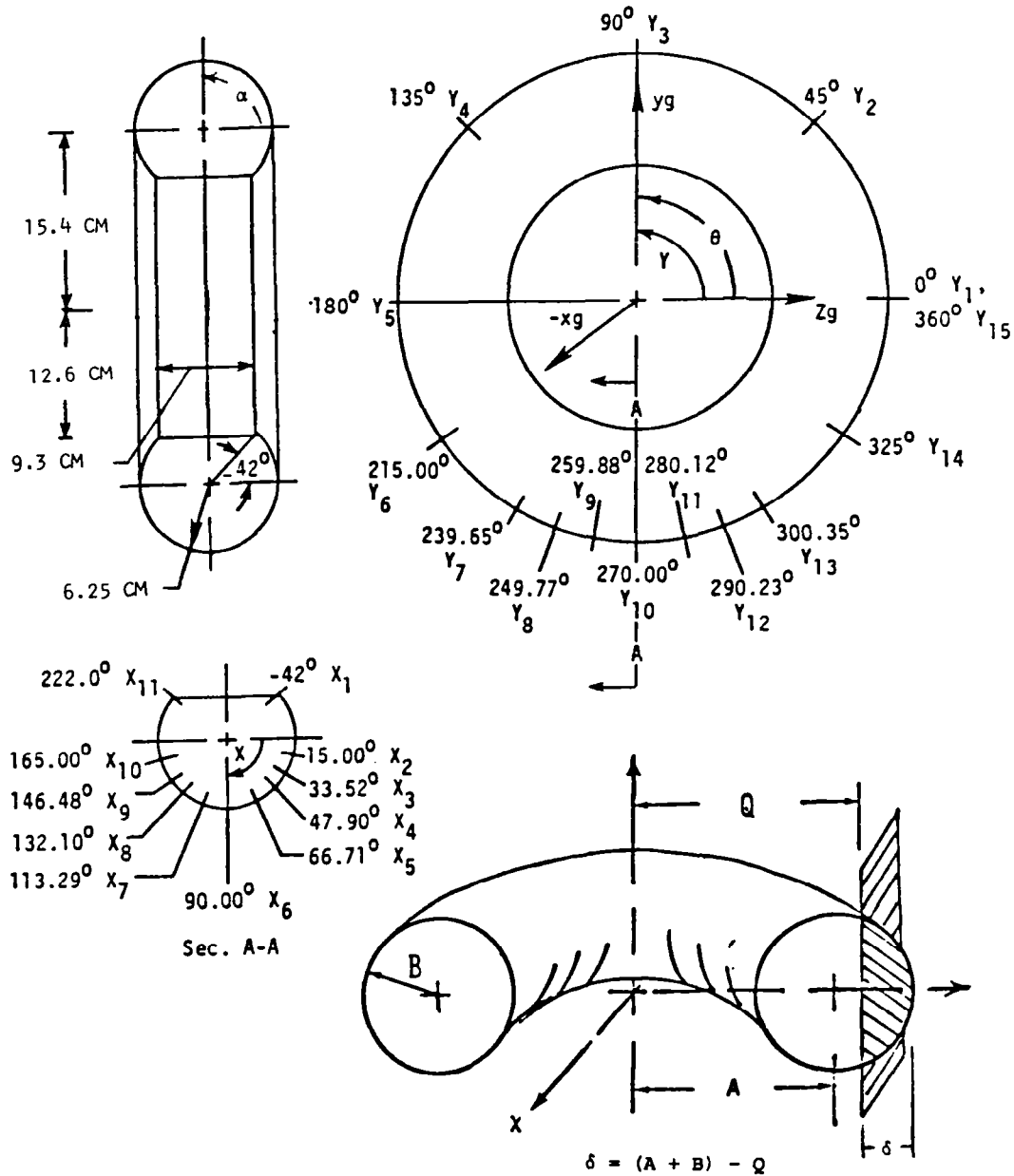
ABSTRACT

Finite element analysis is applied to study the large deflection and stress of a thin-walled pressurized torus loaded by normal contact with a plane. The torus is found to have an elliptical footprint area, and considerable bulge occurs in the sidewall in the vicinity of the load plane. In large load ranges, the finite element calculations show compressive circumferential stress and negative curvature in the footprint region. An experimental study of the standing torus, using liquid metal strain gages, is outlined. Experimentally determined stresses are compared to those resulting from finite element analysis at various meridional and circumferential coordinates of the torus, including the footprint area. Circumferential strains compare favorably while meridional strains are higher in the finite element analysis, probably due to slippage of the boundary at the rim.

This study utilized the STAGS finite element computer program. The purpose of the study was to evaluate the various program options for structural loading, for material modeling, for stress analysis, and for grid refinement. The experimental model, a thin-walled rubber tube mounted on a steel cylindrical rim, provided measured results to compare with various analytical trade-offs. It was found that there was almost no difference in predicted deflections or stress distributions between linear and nonlinear material description. However, the difference between linear analysis and that of geometric nonlinearities utilizing incremental loading was marked.

TORUS DIMENSIONS AND GLOBAL COORDINATE SET

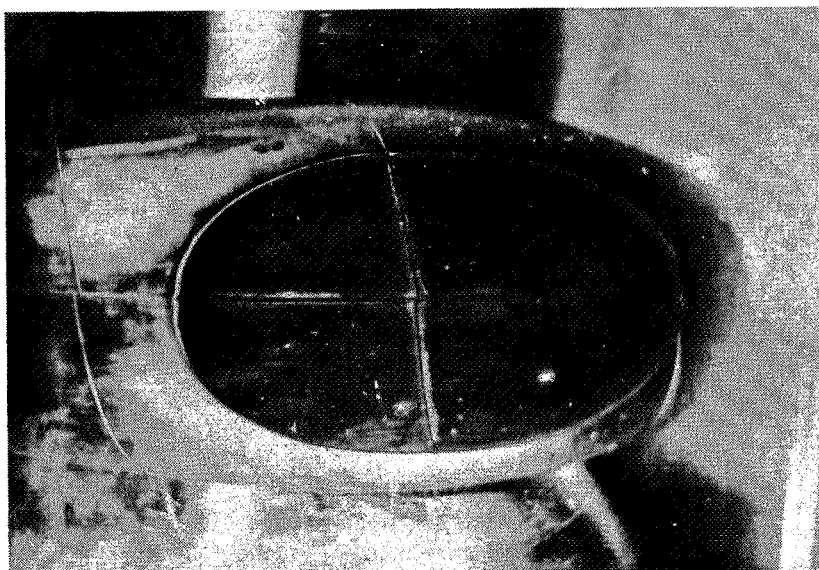
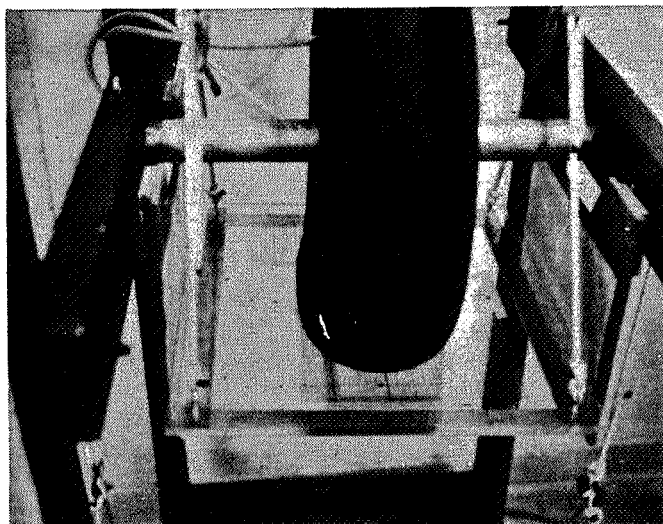
STAGS (ref. 1) uses a first order shell theory to reduce a 3-dimensional structural problem to a dependency on 2 spatial coordinates, here the meridional coordinate α and circumferential coordinate θ . The deflection of the plane into the torus is δ . An example of an 11 x 15 torus grid is shown and dimensions of the cylindrical rim and inflated rubber tube are given.



ORIGINAL PAGE IS
OF POOR QUALITY

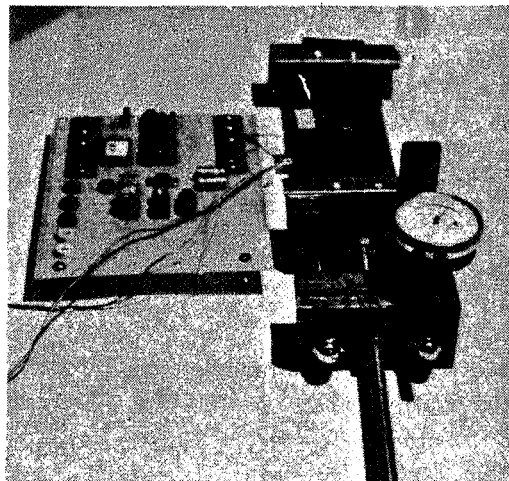
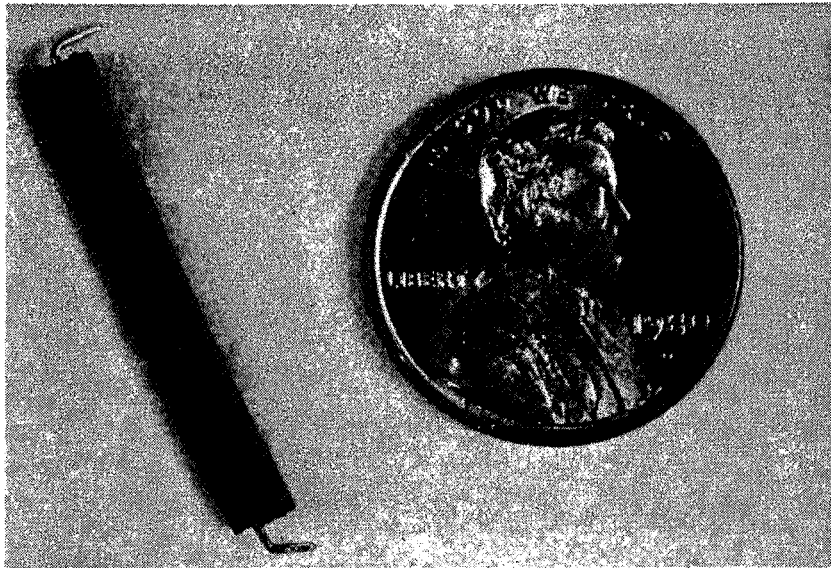
EXPERIMENTAL SET-UP SHOWING ELLIPTICAL FOOTPRINT

The tube was inflated to 0.034 atm. (0.5 psi) and test loads of 34.3 N (7.7 lbs), 69.9 N (15.7 lbs), and 114.4 N (25.7 lbs) were applied. Deflection, footprint area, circumferential and meridional strain, and final pressure were observed.



LIQUID METAL STRAIN GAGE AND CALIBRATION DEVICE

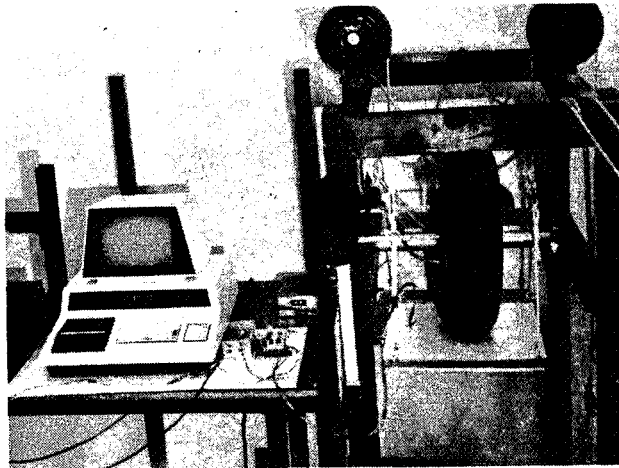
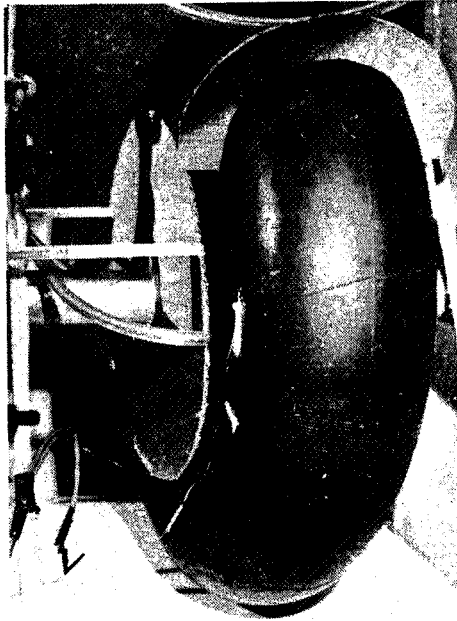
In order to measure the large strain encountered, strain gages with a rubber housing and capillary column of mercury were used. The gages are inherently nonlinear by nature, and individual calibration is required (ref. 2). Derivation of gage factor versus strain is given in the appendix.



GAGE PLACEMENT AT 0° MERIDIONAL ANGLE -
COMPLETE SYSTEM WITH DATA ACQUISITION

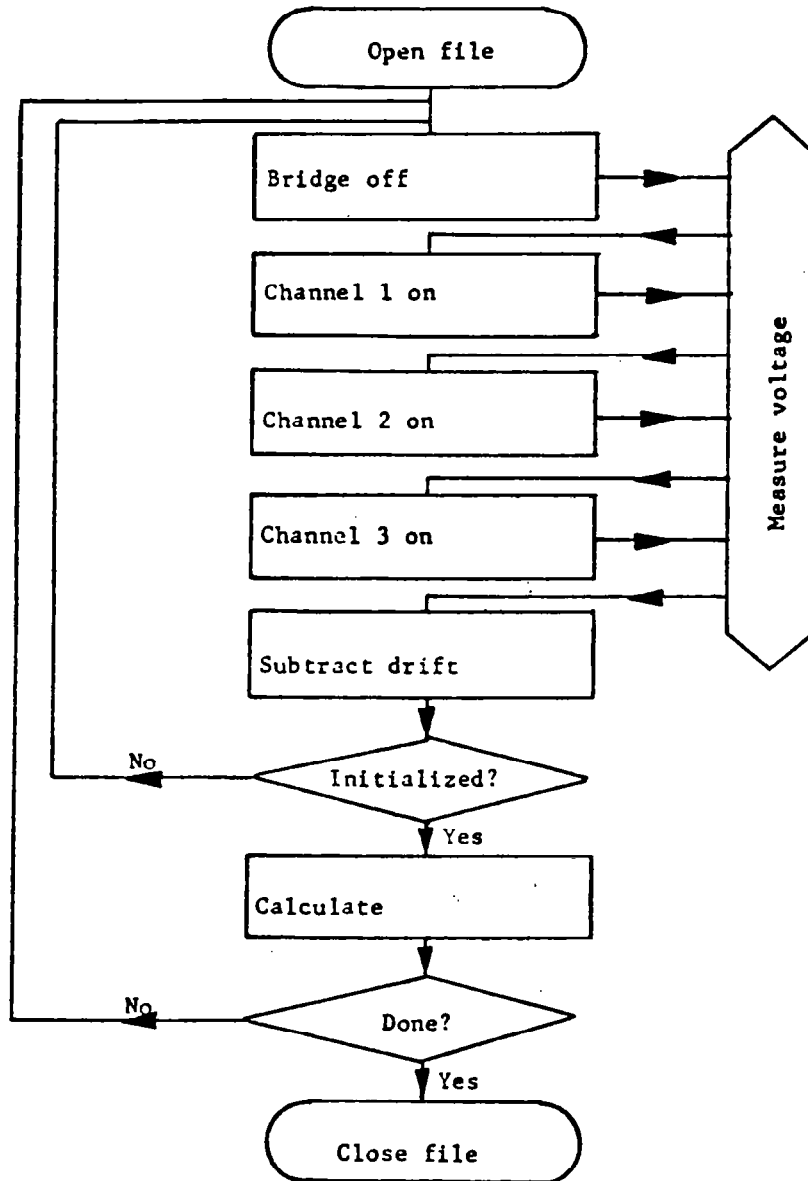
ORIGINAL PAGE IS
OF POOR QUALITY

Calibrated gages were mounted on the torus with silicone rubber cement. The torus was inflated to test pressure and rotated to the desired circumferential angle, load was applied, and readings were recorded. The microprocessor shown below tabulated and recorded, on magnetic tape, data for strain versus circumferential angle at given values of load and meridional angle.



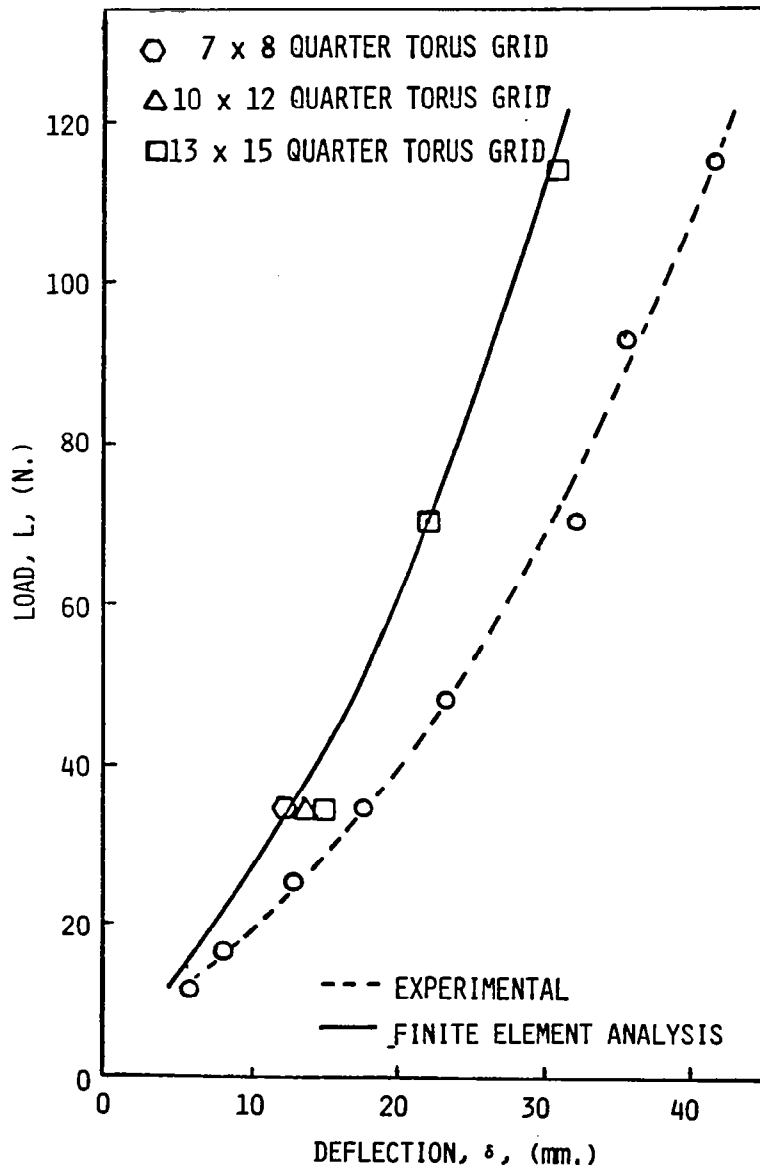
DATA ACQUISITION FLOW CHART

The logic flow chart for the data acquisition scheme is shown below. The buffer for the strain signals and the program controller with the stored logic of the acquisition system are encompassed in the microprocessor. The microprocessor is programmed in the BASIC language, and the digitizing of analog gage voltage is accomplished by a digital voltmeter. The three channels referred to are the meridional strain, the circumferential strain, and a dummy gage voltage.



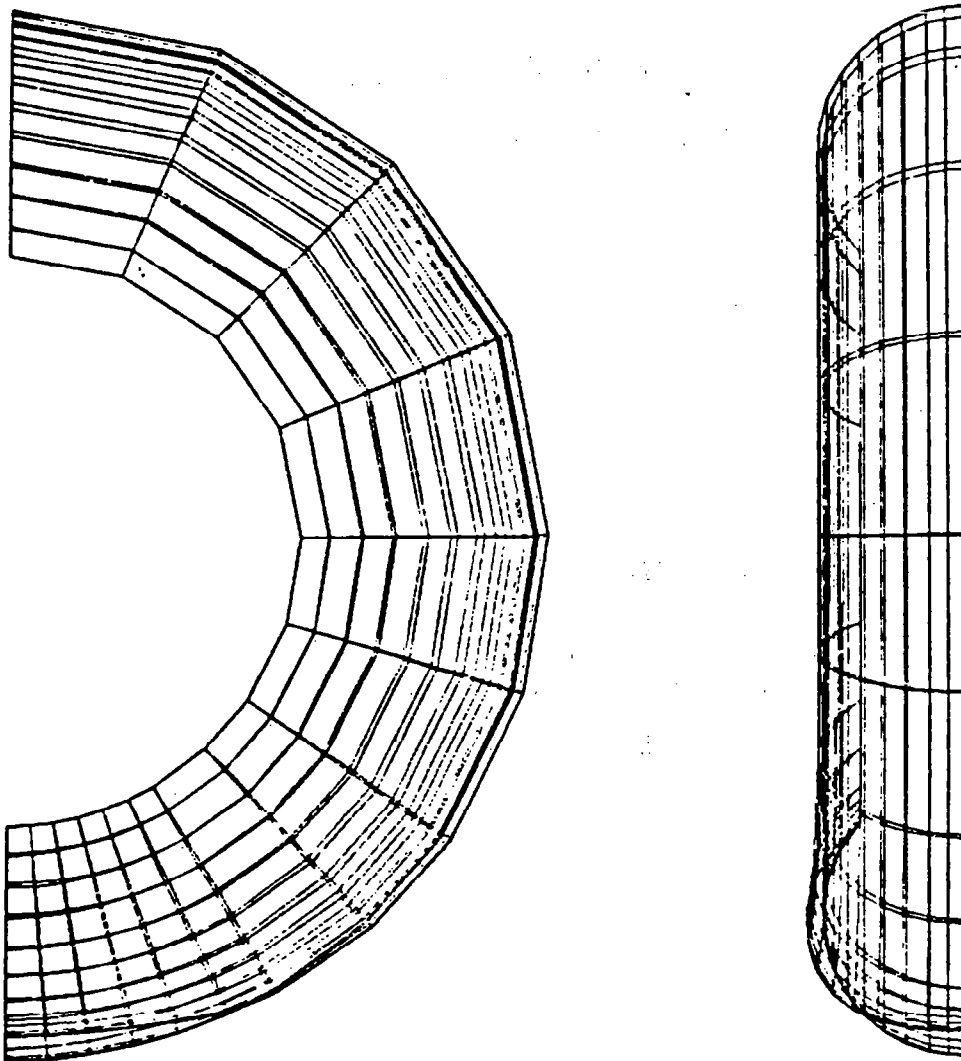
LOAD-DEFLECTION CURVES FOR ANALYTICAL FINITE ELEMENT
AND EXPERIMENTAL DATA FOR TORUS AT $P_1 = 0.034$ ATM

This figure shows points on the load-deflection curve obtained from a STAGS analysis using a 13 x 15 quarter torus at loads of 34.3 N (7.7 lbs), 69.9 N (15.7 lbs), and 114.4 N (25.7 lbs). The deflections predicted from STAGS are lower since minimum potential theory is employed and structural stiffness is overestimated with a coarse grid. As grid size is refined, predicted deflections approach the experimental values, but computer run time also increases (ref. 3). At a load of 34.3 N, three different grid sizes were modeled.



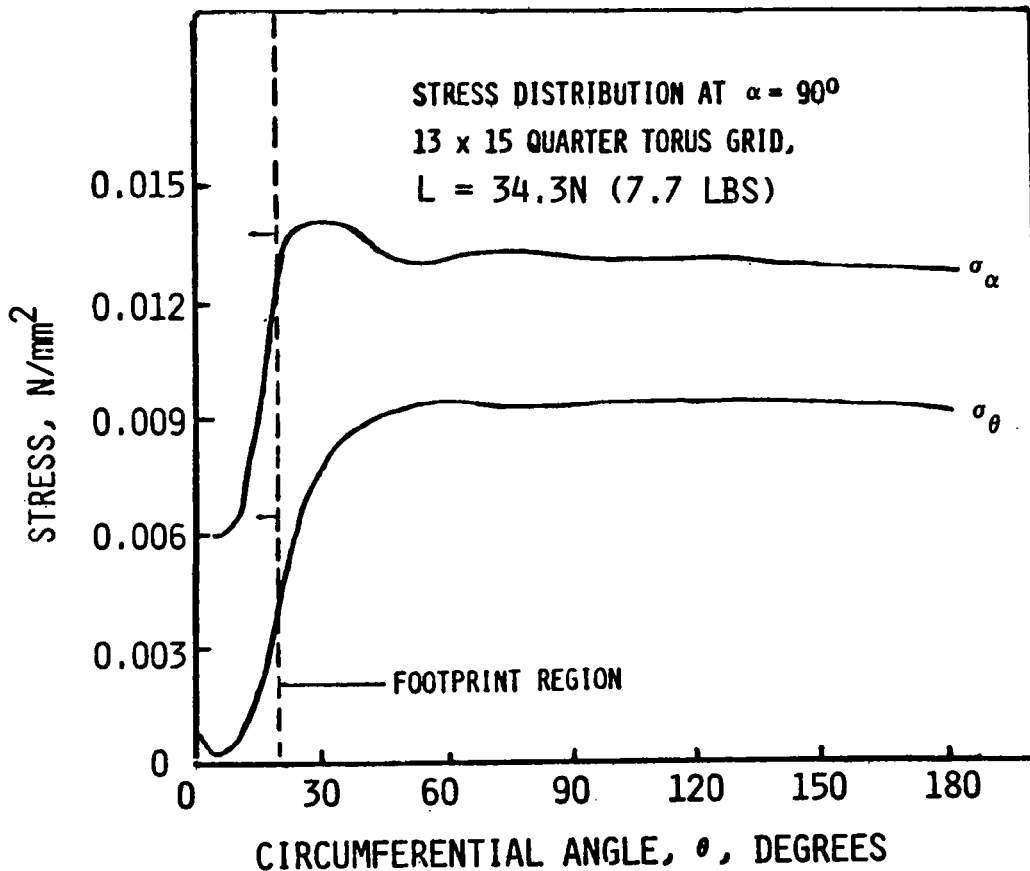
13 x 15 QUARTER TORUS GRIDS WITH
34.3 N (7.7 lbs) LOAD - NONLINEAR ANALYSIS

This figure gives the computer-generated plot of the quarter torus with a 13 x 15 grid. Exploitation of the torus symmetry allows analysis of one-fourth of the structure, giving a grid density four times greater than that of a 13 x 15 grid applied to the full torus. The unloaded grid geometry is overplotted on the the deformed geometry. Note the plane surface at the load point (footprint) and the side wall bulge. The nonlinear geometric analysis option of STAGS gave convergence to a final deflection of 84% of the experimental value while the linear analysis yielded only 21% of the experimental value. This result is significant when compared to toroidal analysis using other finite element procedures (refs. 4 and 5).



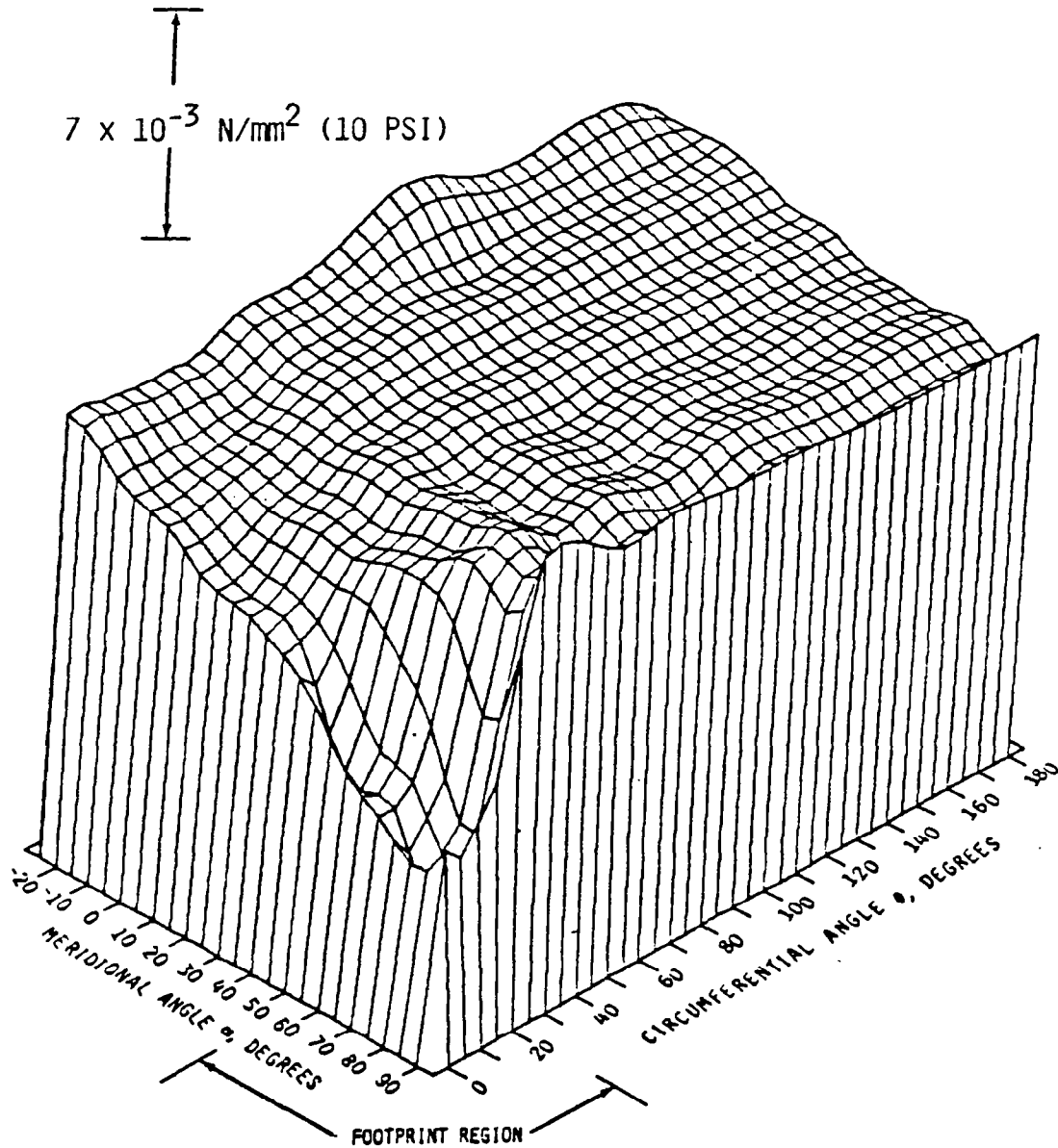
CALCULATED STRESS DISTRIBUTION AT 90° MERIDIONAL
ANGLE FOR 13 x 15 QUARTER TORUS GRID - $L = 34.3 \text{ N}$ (7.7 lbs.)

Calculated values of meridional stress and circumferential stress versus circumferential angle θ are shown below. The variation of stress in the footprint and bulge regions is significant. The values remain constant away from the contact area and are mainly due to internal pressure. These values, with this grid refinement, agree favorably with other investigators (ref. 6).



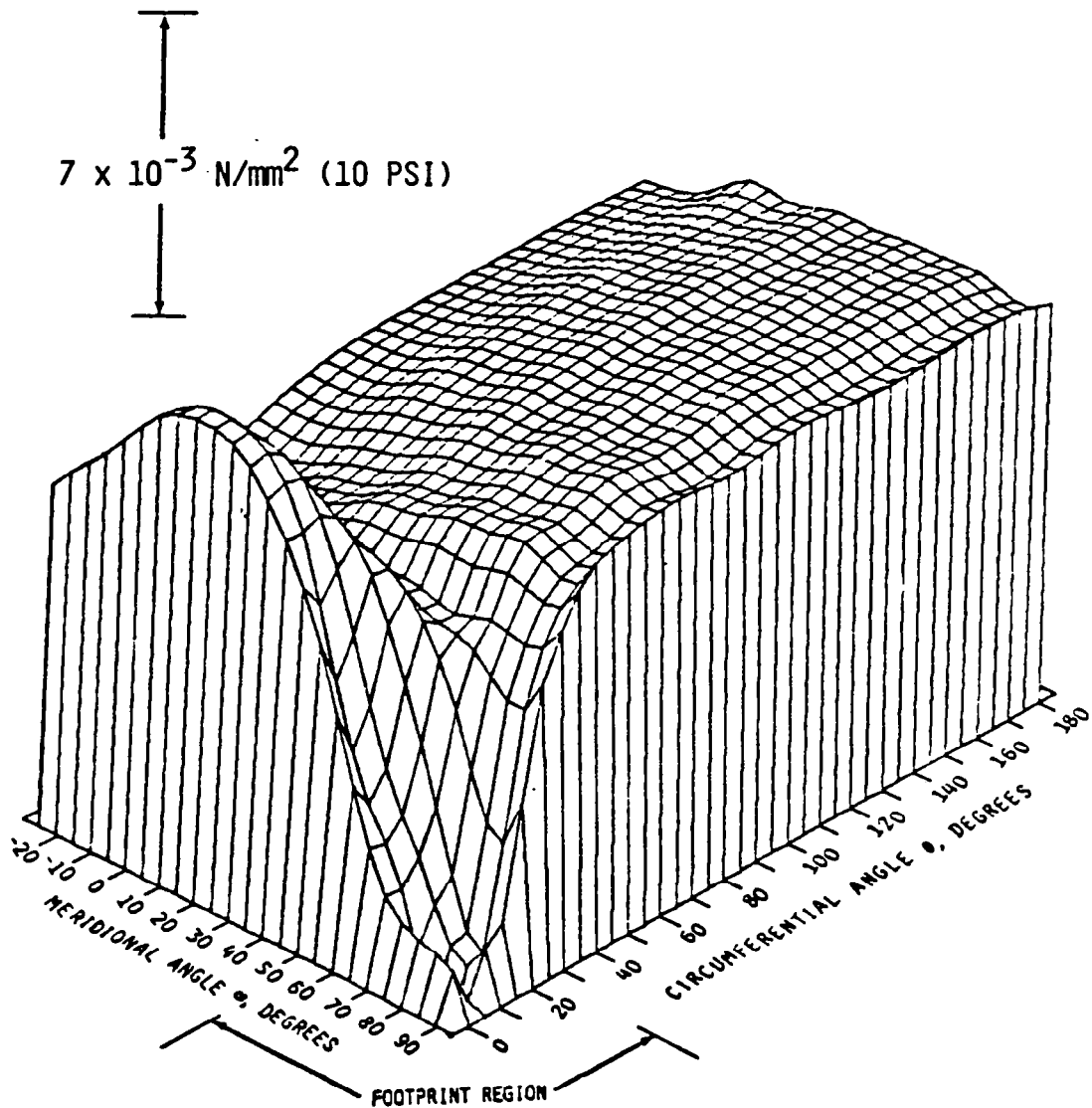
CALCULATED MERIDIONAL STRESS DISTRIBUTION, σ_α , 13 x 15
QUARTER TORUS GRID - NONLINEAR ANALYSIS, LOAD = 34.3 N (7.7 lbs)

The three dimensional plot below shows meridional stress distribution over the surface of the torus at a 34.3 N load. Even tensile stress appears in both the meridional and circumferential directions in the upper half of the torus, as a result of internal gas pressure. However, the compressive effect of contact with the flat plate reduces these tensile stresses in the footprint region.



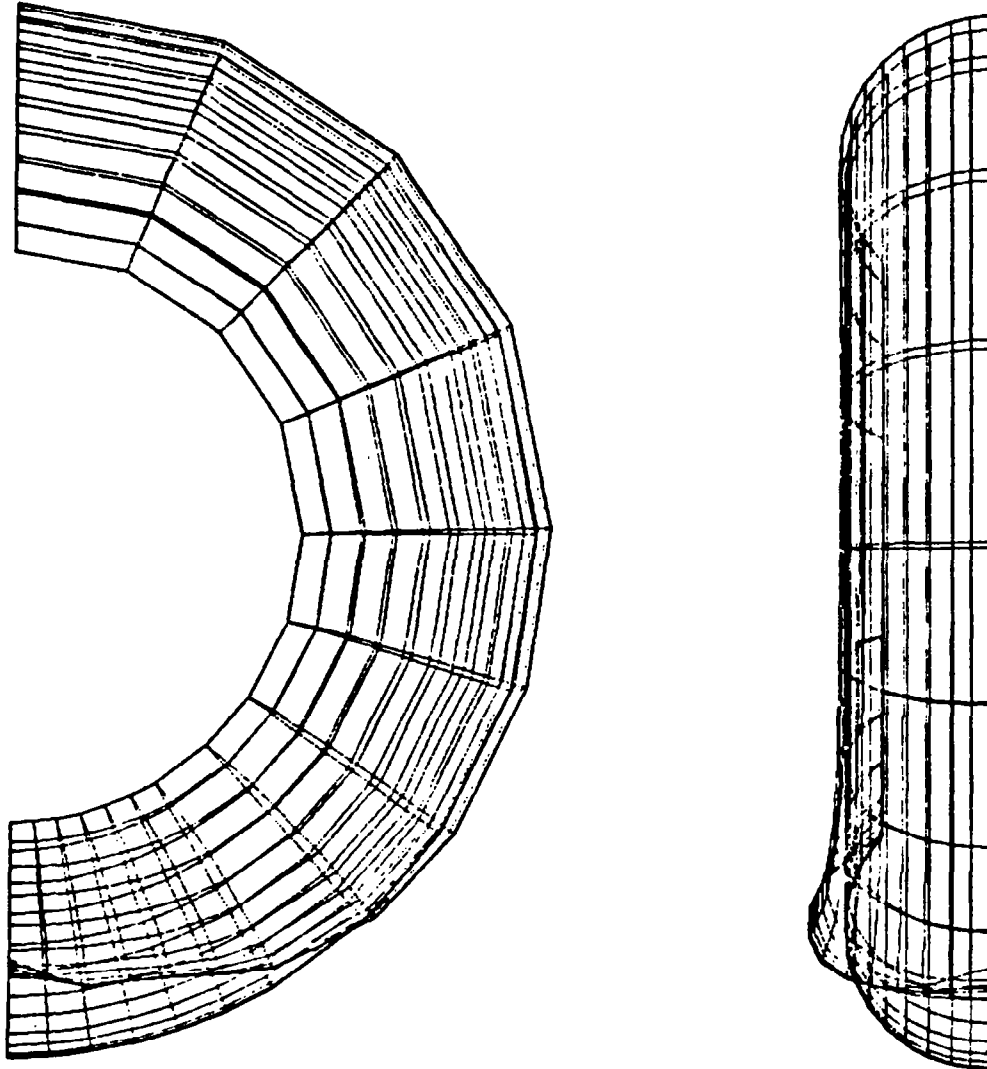
CALCULATED CIRCUMFERENTIAL STRESS DISTRIBUTION, σ_{θ} , 13x15,
QUARTER TORUS GRID - NONLINEAR ANALYSIS, LOAD = 34.3 N (7.7 lbs)

A three dimensional plot of circumferential stress distribution over the upper half of the torus is shown below. As with the previous figure, uniform tensile stress due to gas pressure is significantly reduced in the footprint region, to almost 0 N/mm² in the center. Results of an intermediate load step of 69.9 N (15.7 lbs) are contained in the literature (ref. 7).



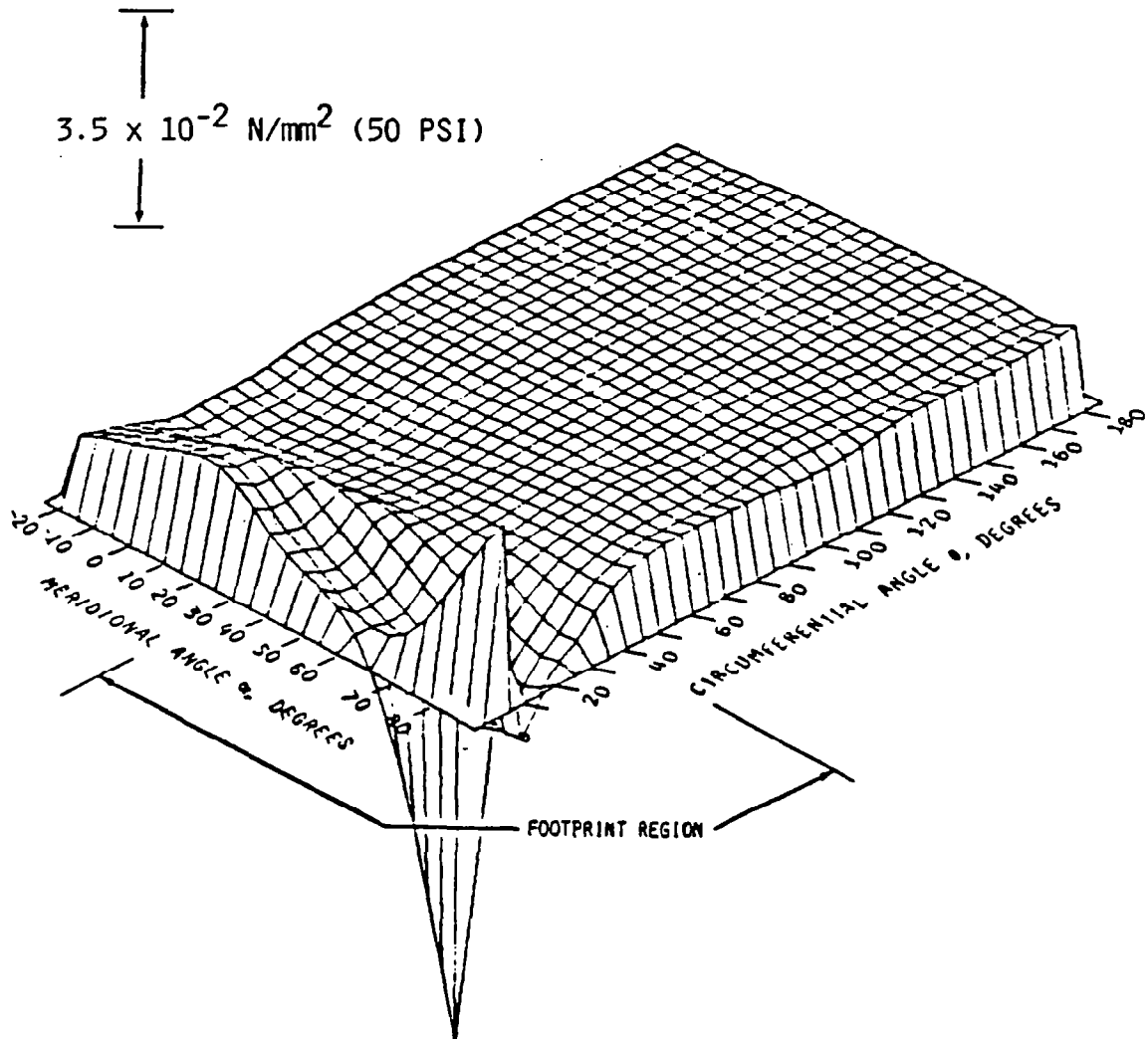
13 x 15 QUARTER TORUS GRID WITH
114.4 N (25.7 lbs) LOAD - NONLINEAR ANALYSIS

The figure below shows the STAGS generated plot of a quarter torus in the unloaded and deformed configurations under a test load of 114.4 N. The deflection has increased significantly and the degree of bulge in the sidewall is more pronounced. The center of the footprint region shows negative curvature.



CALCULATED CIRCUMFERENTIAL STRESS
DISTRIBUTION, σ_θ , AT LOAD = 114.4 N (25.7 lbs.)

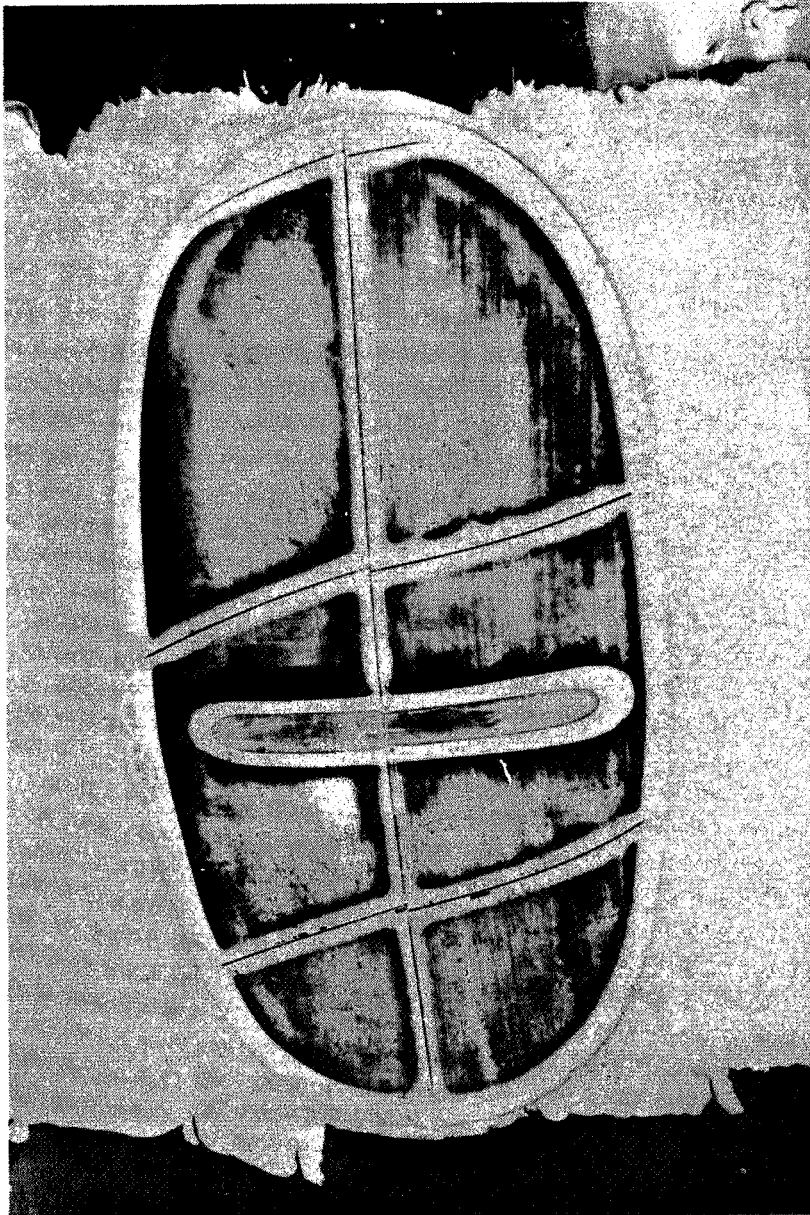
A three dimensional plot of circumferential distribution over the quarter torus is given below for the 114.4 N load. Note the scale change from that of the previous two three dimensional plots. Increased compressive stress in the footprint region is seen to cause a stress reversal in the center of the footprint region. The stress becomes compressive near the center, then suddenly reverses and becomes tensile, suggesting that a local limit point on the structure load deflection path has been reached and snap-through has occurred.



ORIGINAL PAGE IS
OF POOR QUALITY

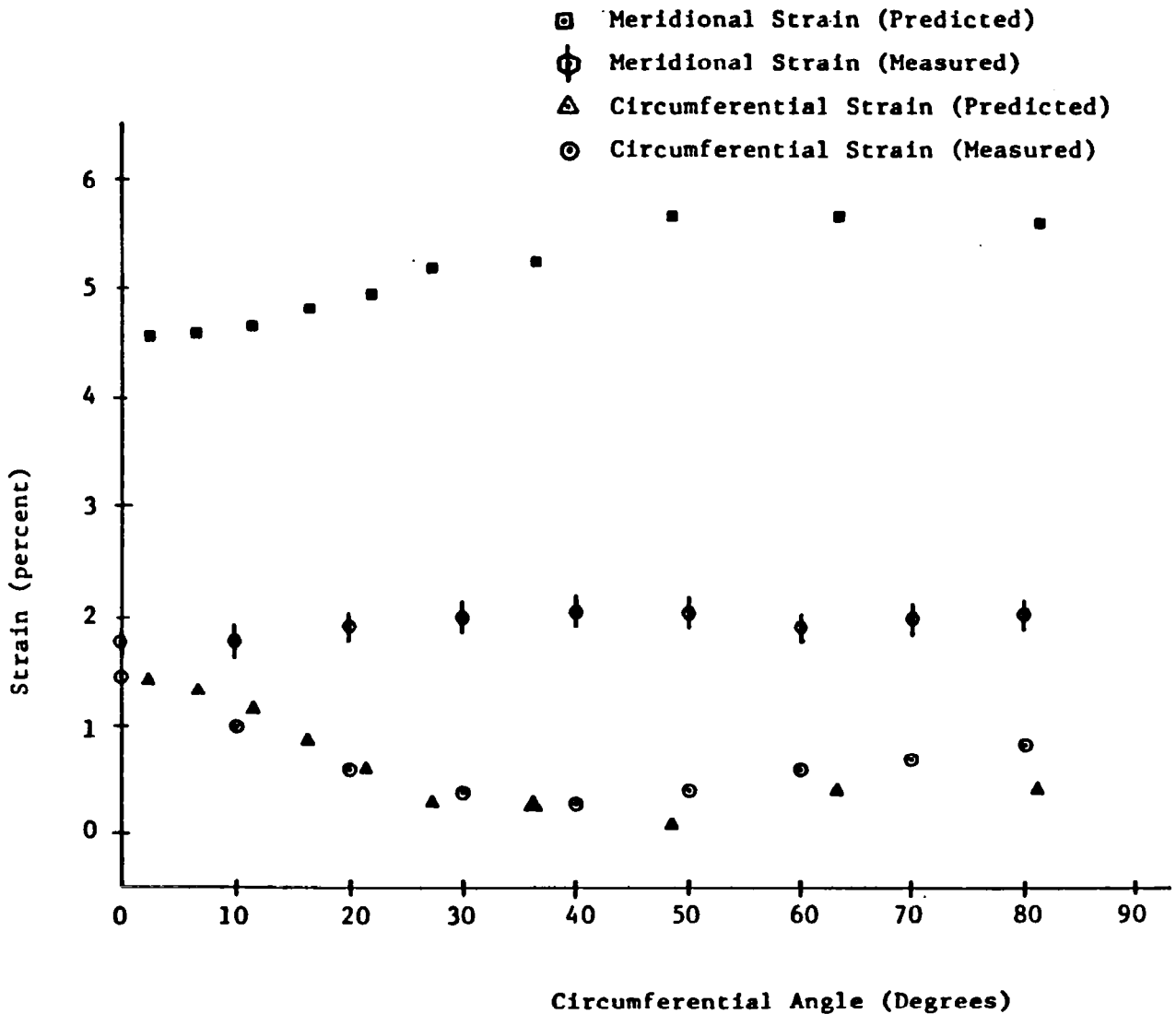
FOOTPRINT OF AN INNER TUBE SHOWING NEGATIVE CURVATURE

The figure below is a photograph of an inner tube under relatively heavy load. An initial eccentricity has been introduced. The negative curvature near the center of the footprint is considerably reduced in the presence of friction at the contacting surfaces (not modeled here).



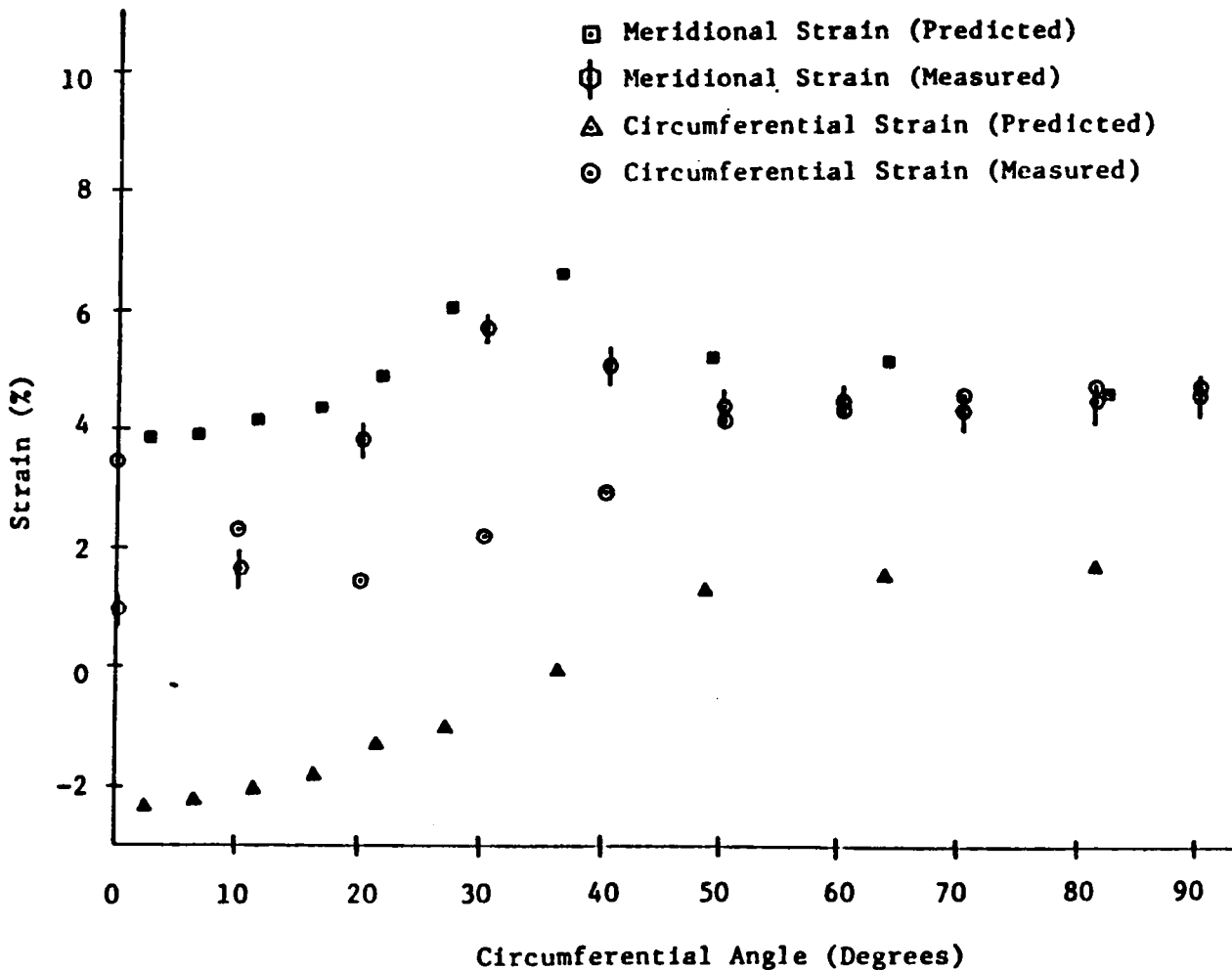
EXPERIMENTAL AND CALCULATED STRAINS AT
-10° MERIDIONAL ANGLE - LOAD = 34.3 N (7.7 lbs.)

The figure below compares measured and calculated meridional and circumferential strains for varying θ at $\alpha = -10^\circ$. This -10° meridional angle places the strain gages in the region near the rim. Good agreement is achieved in observed and calculated values of circumferential strain. The disagreement between observed and calculated meridional strain is attributed to slipping of the membrane under the rim on the test fixture. The computer model had a fixed boundary at the rim.



EXPERIMENTAL AND CALCULATED STRAINS AT
90° MERIDIONAL ANGLE - LOAD = 69.9 N (15.7 lbs.)

This figure compares measured and calculated strains for varying circumferential angle θ at $\alpha = 90^\circ$. At this farthest point from the rim, meridional strains are in good agreement. Note here that for all measurements below $\alpha = 30^\circ$, the strain gage is in the footprint region. Measured strain did not become compressive here, probably due to friction between the contacting surfaces. Reports of strain comparison at other loads are contained in the literature (ref. 8).



REFERENCES

1. Almroth, B. O.; Brogan, F. A.; and Stanley, G. M.: Structural Analysis of General Shells. Vol. 2, Users Instructions for STAGS C-1. LMSC-D 633873, Lockheed-California, April 1979.
2. Hill, D. E.; and Baumgarten, J. R.: The Experimental Stress Analysis of a Thin-Walled Pressurized Torus Loaded by Contact With a Plane. Volume A - Structures and Materials, AIAA/ASME 23rd Structures, Structural Dynamics and Materials Conference May 1982, pp 93 -97.
3. Mack, M. J.; Gassman, P. M.; and Baumgarten, J. R.: The Analysis of a Thin-Walled Pressurized Torus Loaded by Contact with a Plane. Volume A - Structures and Materials, AIAA/ASME 23rd Structures, Structural Dynamics and Materials Conference, May 1982, pp 181 -187.
4. Durand, M.; and Jankovich, E.: Nonapplicability of Linear Finite Element Programs to the Stress Analysis of Tires. NASA TM X-2637, September 1972, pp 263 - 276.
5. Deak, A. L.; and Atluri, S.: The Stress Analysis of Loaded Rolling Aircraft Tires. Vol. 1, Analytical Formulation. AFFDL-TR-73-130, Air Force Flight Dynamics Laboratory, October 1973.
6. DeEskinazi, J.; Soedal, W.; and Yang, T. Y.: Contact of an Inflated Torodial Membrane with a Flat Surface as an Approach to the Tire Deflection Problem. Tire Science and Technology, TSTCA, Vol. 3, February 1975, pp 43 - 61.
7. Mack, M. J.: The Finite Element Analysis of an Inflated Torodial Structure. M. S. Thesis, Iowa State University, 1981.
8. Hill, D. E.: Experimental Stress Analysis of an Inflated Torodial Structure. M. S. Thesis, Iowa State University, 1981.

APPENDIX

In describing the operation of a liquid metal strain gage, one assumes that the liquid metal column obeys the fundamental resistance relation (there are no voids in the column). Further, the resistivity of the conducting medium is assumed constant, and the volume of the capillary cylindrical cavity is assumed constant. Rubber is essentially incompressible; the assumption of constant volume under elongation is a valid one. The fundamental resistance is

$$R = \frac{\rho L}{A} = \frac{\rho L^2}{V} \quad (1)$$

when $\rho \equiv$ resistivity, ohm-in.

$L \equiv$ length, in.

$A \equiv$ cross-sectional area, in.²

$V \equiv$ volume, in.³ = AL

Using a Taylor series expansion about the initial length,

$$\begin{aligned} \Delta R &= \frac{\partial R}{\partial L} (L - L_0) + \frac{\partial^2 R}{\partial L^2} \frac{(L - L_0)^2}{2!} \\ \Delta R &= \frac{\rho}{V} \left[2L_0 (L - L_0) + \frac{2(L - L_0)^2}{2} \right] = \frac{\rho}{V} [2L\Delta L + \Delta L^2] \\ \frac{\Delta R}{R} &= 2 \frac{\Delta L}{L_0} + \frac{\Delta L^2}{L_0^2} = 2\varepsilon + \varepsilon^2 \end{aligned} \quad (2)$$

where $\varepsilon =$ strain, in./in.

Equation 2 establishes a quadratic relationship between resistance change and strain. It is seen from (2) that for small strains, the gage factor is two.